
Some aspects of infinite range models of spin glasses: theory and numerical simulations

Alain Billoire¹

Service de physique théorique, CEA Saclay, 91191 Gif-sur-Yvette FRANCE
billoire@spht.saclay.cea.fr

The expression “spin glasses” was originally coined to describe metallic alloys of a non-magnetic metal with few, randomly substituted, magnetic impurities. Experimental evidences were obtained for a low temperature “spin-glass” phase characterized by a non-periodic freezing of the magnetic moments (the spins) with a very slow, and strongly history dependent, response to external perturbations (this later aspect lead more recently to many fascinating developments). The theoretical analysis of this phenomenon lead to the celebrated Edwards–Anderson model [1] of spin-glasses: classical spins on the sites of a regular lattice with random interactions between nearest neighbor spins. However, after more than thirty years of intense studies, the very nature of the low temperature phase of the Edwards–Anderson model in three dimensions is still debated, even in the simple case of Ising spins. Two main competing theories exist: the mean field approach originating from the work of Sherrington and Kirkpatrick [2], and the so-called “droplet” [3] or scaling theory of spin glasses.

The mean field approach is the application to this problem of the conventional approach to phase transitions in statistical physics: one first builds a mean field theory after identifying the proper order parameter, solve it (usually a straightforward task) and then study the fluctuations around the mean field solution. Usually, fluctuations turn out to have mild effects for space dimensions above the so-called upper critical dimension (up to infinite space dimension, where mean field is exact). Below the upper critical dimension fluctuations have major effects and non-perturbative techniques are needed to handle them. The second item of this agenda (solving the mean field equations) led, with spin glasses, to severe unexpected difficulties, and revealed a variety of new fascinating phenomena. The last step is the subject of the so called “replica field theory”, which is still facing formidable difficulties.

These notes are an introduction to the physics of the infinite range version of the Edwards–Anderson model, the so-called Sherrington–Kirkpatrick model, namely a model of classical spins that are not embedded in Euclidean space, with all pairs of spins interacting with a random interaction. If there is

no more debate whether Parisi famous solution of the Sherrington–Kirkpatrick model in the infinite volume limit is correct, much less is known, as mentioned before, about the Edwards–Anderson model in three dimensions, with numerical simulations as one of our main sources of knowledge. It is accordingly important to test the various methods of analysis proposed for the Edwards–Anderson model, in the Sherrington–Kirkpatrick model case first.

In a first part, I motivate and introduce the Edwards–Anderson and Sherrington–Kirkpatrick models. In the second part, I sketch the analytical solution of the Sherrington–Kirkpatrick model, following Parisi[4, 5, 6, 7]. I next give the physical interpretation of this solution. This is a vast subject, and I concentrate on the major points and give references for more developments. The third part presents the numerical simulation approach and compares some numerical results to theoretical expectations. The last part, more detailed, is about the specific problem of finite size effects for the free energy, which is interesting for both theoretical and practical point of views. I have left aside several very interesting aspects, like the problem of chaos [8, 9] the TAP approach [10] (see [11] for numerical results) and the computation of the complexity [12].

There are many books and review articles about spin glasses and related phenomena: One may start with the text book by Fischer and Hertz [13], the review by Binder and Young [14], which gives a very complete account of the situation in 1986 both experimental, theoretical and numerical with many detailed analytical computations, and (at a higher level) the book by Mézard, Parisi, and Virasoro [15]. More recent references include [16] and [17]. The recent book by de Dominicis and Giardinà [18] gives a very complete exposition of the replica field theory. Reviews on various aspects of the physics of spin glasses can be found in [19, 20, 21]. The non equilibrium behavior of spin glasses have been the subject of intense work during recent years, see [22, 23, 24] for reviews.

1 Introduction

The Edwards–Anderson Ising (EAI) model is the classical Ising model with quenched random interactions. The Hamiltonian is

$$\mathcal{H} = - \sum_{\langle i,j \rangle} J_{i,j} \sigma_i \sigma_j - H \sum_i \sigma_i , \quad (1)$$

where the variables $\sigma_i = \pm 1$ are Ising spins living on the sites of a regular square lattice in d dimensions. H is the magnetic field. The interaction involves all nearest neighbor pairs of spins, with a strength $J_{i,j}$ that depends on the particular link $\langle i, j \rangle$. The $J_{i,j}$'s are quenched variables, namely they do not fluctuate. They have been drawn (once for ever) independently from a unique probability distribution $P(J)$ with mean J_0 and square deviation J^2 . In what

follows, I will consider the case $J_0 = 0$ and choose $J^2 = 1$. The later choice is just the choice of the unit of temperature.

For a fixed set of $J_{i,j}$'s, denoted by \mathcal{J} , one can compute thermodynamic average values, for example the average internal energy $E_{\mathcal{J}} = \langle E \rangle$, where the symbol $\langle \dots \rangle$ denotes the thermodynamics average (with given \mathcal{J}). In general the results depend on \mathcal{J} , and should be averaged over the \mathcal{J} distribution. I note by $\overline{\dots}$ this disorder average.

This model was proposed [1] as a simple model that captures the essential of the physics of spin glasses, and in particular of magnetic spin glasses. Those are alloys with magnetic impurities randomly distributed inside a non magnetic matrix. The interaction between the impurities is the RKKY interaction that oscillates with the distance. Since the positions of the impurities are random, their interactions are random too and one is led to the Edwards-Anderson model (see e.g. [1, 13, 14] for more than this abrupt summary). If this very simple model is to explain convincingly the behavior of real spin glasses, its physics should obviously not depend (too much) on the specific disorder distribution used, as soon as it has zero mean and unit square deviation. This disorder distribution is usually Gaussian (this leads to simpler analytical computations) or binary with values ± 1 (this leads to faster computer programs, using the multi-spin coding technique).

The same model can be generalized to vector spins with two or three components. Those are called the XY and Heisenberg Edwards Anderson models respectively. Most real spin glasses are indeed Heisenberg spin glass with anisotropic interactions (due to the lattice structure, the interaction is not the rotational invariant $\sigma_i \sigma_j$).

In the zero magnetic field case ($H = 0$), there is now an agreement (based mostly on numerical simulations) between spin glass physicists that the EAI model has no transition at finite T in two dimensions, and a transition for three dimensions and above ¹. In the low temperature phase the spins are frozen, with $\langle \sigma_i \rangle \neq 0$, but with a random pattern, and $\sum_i \langle \sigma_i \rangle$ is of order $1/\sqrt{N}$, where N is the number of spins. There is accordingly no spontaneous magnetization. There is no hidden magnetization either: the spins follow no periodic pattern (like e.g. in an anti-ferromagnet), and it is furthermore very likely that the spin orientations are completely reshuffled as soon as one varies the temperature ². This is summarized by the statement: The EAI model is not a disguised ferromagnet.

The statement $\langle \sigma_i \rangle \neq 0$ needs to be made more precise. For a finite system, it means that $\langle \sigma_i \rangle$ is nonzero when observed over a time scale $t \ll t_{erg}(N)$, where $t_{erg}(N)$ is called the ergodic time. At some later time t , the system will eventually tunnel from the current equilibrium state, to a state where $\langle \sigma_i \rangle$ is reversed. However the dynamics of the EAI model is extremely slow and $t_{erg}(N)$ is enormous in the low T phase, as soon as one

¹ The value of the lower critical dimension, between 2 and 3, is not yet settled.

² This is the so called temperature chaos effect.

has few hundred spins, to the point that with any real spin glass, this time is much larger than the duration of any experiment.

In absence of magnetization, we have to find another order parameter for the glass order, one uses the so called Edwards–Anderson parameter, namely

$$q_{EA} = \lim_{t \rightarrow \infty} \lim_{N \rightarrow \infty} \frac{1}{N} \sum_i \langle \sigma_i(t_0) \sigma_i(t + t_0) \rangle, \quad (2)$$

that is nonzero below the spin glass transition and zero above. On a finite system, $C(t) = 1/N \sum_i \langle \sigma_i(t_0) \sigma_i(t + t_0) \rangle$, will rapidly decrease from the starting value $C(1) = 1$, have a plateau of height q_{EA} for a long time (of order t_{erg}) before dropping. As N grows, the plateau becomes longer and longer. The so defined q_{EA} turns out to depend weakly on \mathcal{J} for large systems. This is a so called self averaging quantity (see Subsec 2.3).

One may also consider two independent copies of the system, $\{\sigma_i^{(1)}\}$ and $\{\sigma_i^{(2)}\}$, with the same disorder instance \mathcal{J} (such copies are called real replica, or sometimes clones, in order to distinguish them from the replica of the replica method, see Subsec. 2.2), and consider the probability distribution

$$P_{\mathcal{J}}(q) = \langle \delta(q - \frac{1}{N} \sum_i \sigma_i^{(1)} \sigma_i^{(2)}) \rangle, \quad (3)$$

namely the probability distribution of the overlap $q = 1/N \sum_i \sigma_i^{(1)} \sigma_i^{(2)}$ between the two systems. A nonzero q_{EA} corresponds to two peaks in $P_{\mathcal{J}}(q)$ centered at $q = \pm q_{EA}$. We will see later that, at least for the SK model, $P_{\mathcal{J}}(q)$ has more structure than this double peak.

Clearly, $q_{EA} = \langle M \rangle^2$ for a ferromagnet in d dimensions (still at zero magnetic field), where $\langle M \rangle$ is the spontaneous magnetization. On a finite system, $P(q)$ is made of two Gaussian centered around $\pm \langle M \rangle^2$. Between the two peaks, $P(q)$ is exponentially small [25], of order $\exp(-2\mathcal{A}L^{d-1})$, where \mathcal{A} is the interface tension, and L the linear dimension of the system.

In ferromagnets, the transition happens when the magnetization M acquires a nonzero expectation value, and accordingly the susceptibility $\chi = N \langle M^2 \rangle$ becomes infinite as T decreases towards T_c . In spin glasses the spin susceptibility stays finite as $T \rightarrow T_c$, but the spin-glass susceptibility $\chi_{SG} = N \langle q^2 \rangle$ diverges. There is however a difference: in Ising ferromagnets, one can define a connected susceptibility ³ $N(\langle M^2 \rangle - \langle M \rangle^2)$ that is finite in the low T phase. For Ising spin glasses the analog connected susceptibility diverges, as $N \rightarrow \infty$ in the whole low T phase ⁴

³ In this formula $\langle M \rangle$ is to be interpreted as an average restricted over a time interval of length $\ll t_{erg}(N)$, or simply as $\langle |M| \rangle$.

⁴ It is usually defined as $\sum_{i,j} (\langle \sigma_i \sigma_j \rangle - \langle \sigma_i \rangle \langle \sigma_j \rangle)^2$, sometimes simply as $N(\langle q^2 \rangle - \langle q \rangle^2)$.

2 The Sherrington–Kirkpatrick model

This model [2] is a simplified version of the Edwards–Anderson model, where all spins are directly coupled. The Hamiltonian is

$$\mathcal{H} = - \sum_{1 \leq i < j \leq N} \frac{J_{i,j}}{\sqrt{N}} \sigma_i \sigma_j - H \sum_i \sigma_i, \quad (4)$$

where N is the number of spins. The $J_{i,j}$'s are again drawn from a unique probability distribution $P(\mathcal{J})$ with zero mean and unit square deviation. The factor $1/\sqrt{N}$ will ensure a finite limit for the internal energy per spin $e_N(T)$ as $N \rightarrow \infty$. It is in some sense a model in infinite dimension since a given spin is coupled to N spins, with $N \rightarrow \infty$ in the thermodynamic limit. The model has “infinite connectivity”. The infinite connectivity will ensure that the mean field method gives the exact result. As we will show, the SK model can be solved exactly in the thermodynamic limit, and the result is independent of the choice made for the disorder distribution $P(\mathcal{J})$.

The standard method to solve this model is the famous replica trick⁵. One is interested in computing the average free energy $-\beta F_{\mathcal{J}} = \overline{\ln Z_{\mathcal{J}}}$, where $\beta = 1/T$ is the inverse temperature, in units such that $k_B = 1$. This is done by considering the partition function of n identical un-coupled copies of the system, with the same instance of the disorder \mathcal{J} . Such copies are called replica. The partition function is simply the n th power of $Z_{\mathcal{J}}$, $Z_{\mathcal{J}}^n$. Continuing this function defined for integer $n \geq 1$ to a function of the real variable n , one has, at least for finite N ,

$$-\beta F = \overline{\ln Z_{\mathcal{J}}} = \lim_{n \rightarrow 0} \frac{\overline{Z_{\mathcal{J}}^n} - 1}{n}. \quad (5)$$

$Z_{\mathcal{J}}^n$ can be written as

$$\begin{aligned} Z_{\mathcal{J}}^n &= \text{Tr}_{\sigma}^{[n]} \exp(-\beta(\mathcal{H}_{\mathcal{J}}^{[n]})) \\ &= \text{Tr}_{\sigma}^{[n]} \exp(-\beta(\mathcal{H}_{\mathcal{J}}(\sigma^{(1)}) + \dots + \mathcal{H}_{\mathcal{J}}(\sigma^{(n)}))), \end{aligned} \quad (6)$$

where $\sigma^{(1)}$ represents the N spins of the first replica (namely $\{\sigma_i^{(1)}\}$), $\sigma^{(2)}$ the N spins of the second replica, \dots , and $\text{Tr}_{\sigma}^{[n]}$ is the trace over the nN spin variables. The average over the $n(n-1)/2$ $J_{i,j}$ variables are independent, and the disorder average factorizes as a product of terms of the form

$$\overline{\exp\left(\frac{\beta J_{i,j} X_{i,j}}{\sqrt{N}}\right)} = \exp\left(\sum_{p=1}^{\infty} \frac{\beta^p X_{i,j}^p [J]_p}{p! N^{p/2}}\right), \quad (7)$$

⁵ There is an alternative method called the cavity method, see [15, 26].

where

$$X_{i,j} = \sigma_i^{(1)} \sigma_j^{(1)} + \sigma_i^{(2)} \sigma_j^{(2)} + \dots + \sigma_i^{(n)} \sigma_j^{(n)} = \sum_{a=1}^n \sigma_i^{(a)} \sigma_j^{(a)}, \quad (8)$$

and the $[J]_p$'s are the successive cumulants of the disorder distribution $P(\mathcal{J})$,

$$\begin{aligned} [J]_1 &= \overline{J} \\ [J]_2 &= \overline{(J - \overline{J})^2} \\ [J]_3 &= \overline{(J - \overline{J})^3} \\ [J]_4 &= \overline{(J - \overline{J})^4} - 3\overline{(J - \overline{J})^2}^2 \\ &\dots \end{aligned} \quad (9)$$

Since we have $\overline{J} = 0$ and $\overline{J^2} = 1$, one is led to the result

$$\overline{\exp\left(\frac{\beta J_{i,j} X_{i,j}}{\sqrt{N}}\right)} = \exp\left(\frac{\beta^2 X_{i,j}^2}{2N} + \dots\right). \quad (10)$$

The neglected terms in the exponent are of order $1/N^2$ and will not contribute to the thermodynamics limit ⁶, and accordingly the physics is independent of the disorder distribution. One obtains for the disorder averaged partition function:

$$\begin{aligned} \overline{Z_{\mathcal{J}}^n} &= Tr_{\sigma}^{[n]} \exp\left(\frac{\beta^2}{2N} \sum_{i < j} \left(\sum_{b=1}^n \sigma_i^{(b)} \sigma_j^{(b)}\right)^2 + \beta H \sum_i \sum_{b=1}^n \sigma_i^{(b)}\right) \\ &= Tr_{\sigma}^{[n]} \exp\left(\frac{\beta^2}{2N} \sum_{a < b} \sum_i \left(\sum_i \sigma_i^{(a)} \sigma_i^{(b)}\right)^2 + \beta H \sum_i \sum_{b=1}^n \sigma_i^{(b)}\right) \\ &\quad + (nN - n^2) \frac{\beta^2}{4}. \end{aligned} \quad (11)$$

The average over the disorder has been performed analytically, but now the n replicas are coupled. In order to proceed further, one uses the formula

$$\sqrt{\frac{N\beta^2}{2\pi}} \int_{-\infty}^{+\infty} dq \exp\left(-\frac{N\beta^2 q^2}{2}\right) \exp(q\beta^2 X) = \exp\left(\frac{\beta^2 X^2}{2N}\right), \quad (12)$$

introducing $n(n-1)/2$ auxiliary real variables $q_{a,b}$ ($a < b$), with the result

⁶ They are altogether absent if the distribution is Gaussian.

$$\begin{aligned} \overline{Z_{\mathcal{J}}^n} &= \left[\prod_{a < b} \sqrt{\frac{N\beta^2}{2\pi}} \int dq_{a,b} \right] \text{Tr}_{\sigma}^{[n]} \exp\left(-\frac{N\beta^2}{2} \sum_{a < b} q_{a,b}^2 \right. \\ &\quad \left. + \beta^2 \sum_{a < b} q_{a,b} \sum_i \sigma_i^{(a)} \sigma_i^{(b)} + \beta H \sum_i \sum_{b=1}^n \sigma_i^{(b)} + (nN - n^2) \frac{\beta^2}{4} \right). \end{aligned} \quad (13)$$

The variables $q_{a,b}$ have been defined for $a < b$. In the following, it will be sometimes convenient to define $q_{a,b}$ for $a \geq b$ also, as $q_{a,b} = q_{b,a}$ and $q_{a,a} = 0$. For a given replica index a , the trace over the spins factorizes as

$$\begin{aligned} &\prod_{i=1}^N \text{Tr}_{\sigma_i^{(a)}} e^{\beta^2 \sum_{a < b} q_{a,b} \sum_i \sigma_i^{(a)} \sigma_i^{(b)} + \beta H \sum_i \sum_{b=1}^n \sigma_i^{(b)}} \\ &= \left(\text{Tr}_{S^{(a)}} e^{\beta^2 \sum_{a < b} q_{a,b} S^{(a)} S^{(b)} + \beta H \sum_{b=1}^n S^{(b)}} \right)^N, \end{aligned} \quad (14)$$

where $S^{(a)}$ is any of the $\sigma_i^{(a)}$'s, or alternatively the spin of a single spin system, which is replicated n times. Thus ⁷

$$\begin{aligned} \overline{Z_{\mathcal{J}}^n} &= \left[\prod_{a < b} \sqrt{\frac{N\beta^2}{2\pi}} \int dq_{a,b} \right] \exp\left(-\frac{N\beta^2}{2} \sum_{a < b} q_{a,b}^2 \right. \\ &\quad \left. + N \log\left(\text{Tr}_S^{[n]} \left[\exp\left(\beta^2 \sum_{a < b} q_{a,b} S^{(a)} S^{(b)} + \beta H \sum_{b=1}^n S^{(b)}\right)\right]\right) + nN \frac{\beta^2}{4} \right). \end{aligned} \quad (15)$$

The formula has a particularly simple form, with all dependence in N explicit

$$\overline{Z_{\mathcal{J}}^n} = \left[\prod_{a < b} \sqrt{\frac{N\beta^2}{2\pi}} \int dq_{a,b} \right] \exp(-N\beta\mathcal{A}(\{q_{a,b}\})). \quad (16)$$

Up to now our derivation is exact (for a Gaussian disorder) in the $n \rightarrow 0$ limit. We now make the saddle point (or steepest descent) approximation, which gives the correct $N \rightarrow \infty$ behavior. Assuming the existence of a unique absolute maximum of the integrand at location $\{q_{a,b}^{SP}\}$, one has

$$\overline{Z_{\mathcal{J}}^n} \approx \exp(-N\beta\mathcal{A}(\{q_{a,b}^{SP}\})). \quad (17)$$

⁷ From now on, we omit the n^2 terms in the exponent, since they do not contribute in the $n \rightarrow 0$ limit.

By assumption, all partial derivatives of \mathcal{A} , $\partial\mathcal{A}/\partial q_{a,b}$, are zero at the saddle point, and the matrix of the second derivatives, the Hessian, has only nonnegative eigenvalues. The free energy of the original SK model is thus simply related to the saddle point of the $q_{a,b}$ integral representation of the partition function of the n times replicated model (with a reckless interchange of limits),

$$f = \lim_{N \rightarrow \infty} \frac{F}{N} = \lim_{n \rightarrow 0} \frac{1}{n} \mathcal{A}(\{q_{a,b}^{SP}\}) . \quad (18)$$

Note that the saddle point equations can be written as self consistent equations, involving a single spin system

$$q_{a,b}^{(SP)} = \frac{\text{Tr}_S[S^{(a)}S^{(b)} \exp(\beta^2 \sum_{a<b} q_{a,b}^{(SP)} S^{(a)}S^{(b)} + \beta H \sum_{b=1}^n S^{(b)})]}{\text{Tr}_S[\exp(\beta^2 \sum_{a<b} q_{a,b}^{(SP)} S^{(a)}S^{(b)} + \beta H \sum_{b=1}^n S^{(b)})]} . \quad (19)$$

The replica method is not limited to the evaluation of the free energy. It can be used to compute the average (thermodynamic average and disorder average) of any function of the spins. Let $\mathcal{O}(\sigma)$ be a function of the spins $\{\sigma_i\}$, we have by definition, for any disorder sample:

$$\langle \mathcal{O}(\sigma) \rangle = \frac{\text{Tr}_\sigma^{[1]} \mathcal{O}(\sigma^{(1)}) \exp(-\beta(\mathcal{H}_J^{[1]}))}{Z_J} . \quad (20)$$

Multiplying both numerator and denominator by Z^{n-1} , and letting ⁸ $n \rightarrow 0$, we have

$$\langle \mathcal{O}(\sigma) \rangle = \lim_{n \rightarrow 0} \text{Tr}_\sigma^{[n]} \mathcal{O}(\sigma^{(1)}) \exp(-\beta(\mathcal{H}_J^{[n]})) . \quad (21)$$

The right hand side is of a form whose disorder average is readily computed using (10). The method is extended readily to the disorder average of products like $\langle \mathcal{O}(\sigma) \rangle \langle \mathcal{P}(\sigma) \rangle$. Introducing two real replica, we have indeed

$$\langle \mathcal{O}(\sigma) \rangle \langle \mathcal{P}(\sigma) \rangle = \frac{\text{Tr}_\sigma^{[2]} \mathcal{O}(\sigma^{(1)}) \mathcal{P}(\sigma^{(2)}) \exp(-\beta(\mathcal{H}_J^{[2]}))}{Z_J^2} . \quad (22)$$

Multiplying both numerator and denominator by Z^{n-2} , and letting $n \rightarrow 0$, we have

$$\langle \mathcal{O}(\sigma) \rangle \langle \mathcal{P}(\sigma) \rangle = \lim_{n \rightarrow 0} \text{Tr}_\sigma^{[n]} \mathcal{O}(\sigma^{(1)}) \mathcal{P}(\sigma^{(2)}) \exp(-\beta(\mathcal{H}_J^{[n]})) . \quad (23)$$

which is again of a form whose disorder average is readily computed using (10).

⁸ We did add $n - 1$ replica to the one real replica and then let $n \rightarrow 0$.

2.1 Interpretation of the $q_{a,b}$ variables

The $q_{a,b}$ variables have been introduced formally. Their value at the saddle point has a simple interpretation [27] in terms of the overlaps between real replicas as defined in (3). Consider two clones $\sigma^{(1)}$ and $\sigma^{(2)}$ and compute the generating function $G(y)$ ⁹.

$$G(y) = \overline{\left\langle \exp\left(\frac{y\beta^2}{N} \sum_i \sigma_i^{(1)} \sigma_i^{(2)}\right) \right\rangle}. \quad (24)$$

We have,

$$\left\langle e^{\frac{y\beta^2}{N} \sum_i \sigma_i^{(1)} \sigma_i^{(2)}} \right\rangle = \frac{1}{Z^2} \text{Tr}_\sigma^{(2)} e^{\frac{y\beta^2}{N} \sum_i \sigma_i^{(1)} \sigma_i^{(2)} - \beta \mathcal{H}_J^{[2]}}. \quad (25)$$

Multiplying the numerator and denominator by Z^{n-2} , and letting $n \rightarrow 0$, one obtains after averaging over the disorder

$$G(y) = Z^{-n} \left[\prod_{a<b} \sqrt{\frac{N\beta^2}{2\pi}} \int dq_{a,b} \right] \exp\left(y\beta^2 q_{1,2} - \frac{N\beta^2}{2} \sum_{a<b} q_{a,b}^2 \right) \quad (26)$$

$$+ N \log\left(\text{Tr}_S^{[n]} \left[\exp\left(\beta^2 \sum_{a<b} q_{a,b} S^{(a)} S^{(b)} + \beta H \sum_{b=1}^n S^{(b)} \right) \right] + nN \frac{\beta^2}{4} \right),$$

with $Z^n = 1$ since $n \rightarrow 0$.

At leading order in $1/N$, the saddle point is y independent, and accordingly

$$\overline{\left\langle \exp\left(\frac{y\beta^2}{N} \sum_i \sigma_i^{(1)} \sigma_i^{(2)}\right) \right\rangle} = \exp(y\beta^2 q_{1,2}^{SP}). \quad (27)$$

If the saddle point is not symmetric, namely if the $q_{a,b}^{SP}$'s are not all equal, the solution of the saddle point equations is degenerate, and one must average¹⁰ over all degenerate solutions, or alternatively all permutations of a and b . The correct formula is then

$$\overline{\left\langle \exp\left(\frac{y\beta^2}{N} \sum_i \sigma_i^{(1)} \sigma_i^{(2)}\right) \right\rangle} = \frac{2}{n(n-1)} \sum_{a<b} \exp(y\beta^2 q_{a,b}^{SP}), \quad (28)$$

where $n(n-1)/2$ is the number of $q_{a,b}$ variables. This implies the following direct relation between the disorder averaged $P(q)$ and the value of $q_{a,b}$ at the saddle point

⁹ This is a convenient way to evaluate at once the expression $\overline{\left\langle (1/N \sum_i \sigma_i^{(1)} \sigma_j^{(2)})^k \right\rangle}$ for all values of k .

¹⁰ Since the saddle point solution is degenerate, one must sum over the solutions in both numerators and denominators of (26).

$$\begin{aligned}
P(q) &= \overline{P(q)}_{\mathcal{J}} = \overline{\left\langle \delta\left(q - \frac{1}{N} \sum_i \sigma_i^{(1)} \sigma_i^{(2)}\right) \right\rangle} \\
&= \frac{2}{n(n-1)} \sum_{a < b} \delta(q - q_{a,b}^{SP}).
\end{aligned} \tag{29}$$

The distribution $P_{\mathcal{J}}(q)$, namely before disorder average, has an interpretation in terms of pure states. In the rigorous formulation of statistical physics (without disorder), pure states give a precise definition of thermodynamic phases directly in the infinite volume limit (see [21] for a discussion from a physicist point of view). Pure states have the following properties:

- The clustering property: Inside a pure state, spin correlation functions factorize when the distance goes to infinity. For example if α is a pure state, one has $\langle \sigma_x \sigma_y \rangle_{\alpha} \rightarrow \langle \sigma_x \rangle_{\alpha} \langle \sigma_y \rangle_{\alpha}$, as $|x - y| \rightarrow \infty$.
- Every translationally invariant state is a convex linear combination of pure states. This means that for any A , one has $\langle A \rangle = \sum_{\alpha} w_{\alpha} \langle A \rangle_{\alpha}$, where the weights $w_{\alpha} \geq 0$, with $\sum_{\alpha} w_{\alpha} = 1$, are independent of A .

In a ferromagnet at temperature $T < T_c$, there are two T -dependent pure states corresponding to states with positive and negative magnetizations respectively, that we can call the “+” and the “-” states. A general translationally invariant state is a linear combination of these two pure states. For example, doing the infinite volume limit (at zero magnetic field) by considering a set of finite systems of increasing sizes with periodic boundary conditions, one has $\omega_+ = \omega_- = 1/2$.

Let us assume (departing boldly from rigor) that the same decomposition holds for finite systems in the SK model for every disorder sample, namely that $\langle A \rangle = \sum_{\alpha} w_{\alpha} \langle A \rangle_{\alpha}$, for any A , where the weights and the states are (disorder) sample dependent. We introduce \mathcal{Q} , the overlap between two pure states.

$$\mathcal{Q}_{\alpha,\beta} = \frac{1}{N} \sum_i \langle \sigma_i^{(1)} \rangle_{\alpha} \langle \sigma_i^{(2)} \rangle_{\beta}. \tag{30}$$

In a ferromagnet $\mathcal{Q}_{+,+} = \mathcal{Q}_{-,-} = \langle M \rangle^2$, and $\mathcal{Q}_{+,-} = \mathcal{Q}_{-,+} = -\langle M \rangle^2$. We now proceed to show that the overlap between pure states is related to the clone overlap introduced in (3). We do this by considering successive moments of q . For the first moment, we have

$$\begin{aligned}
\langle q \rangle &= \frac{1}{N} \sum_i \langle \sigma_i^{(1)} \sigma_i^{(2)} \rangle \\
&= \frac{1}{N} \sum_i \langle \sigma_i^{(1)} \rangle \langle \sigma_i^{(2)} \rangle,
\end{aligned} \tag{31}$$

since $\sigma^{(1)}$ and $\sigma^{(2)}$ are independent systems. Introducing the pure states, this gives

$$\begin{aligned} \langle q \rangle &= \frac{1}{N} \sum_i \sum_{\alpha, \beta} \omega_\alpha \omega_\beta \langle \sigma_i^{(1)} \rangle_\alpha \langle \sigma_i^{(2)} \rangle_\beta \\ &= \sum_{\alpha, \beta} \omega_\alpha \omega_\beta \mathcal{Q}_{\alpha, \beta} . \end{aligned} \quad (32)$$

For the second moment we have

$$\begin{aligned} \langle q^2 \rangle &= \frac{1}{N^2} \sum_i \sum_j \langle \sigma_i^{(1)} \sigma_j^{(1)} \sigma_i^{(2)} \sigma_j^{(2)} \rangle \\ &= \frac{1}{N^2} \sum_{i, j} \langle \sigma_i^{(1)} \sigma_j^{(1)} \rangle \langle \sigma_i^{(2)} \sigma_j^{(2)} \rangle \\ &= \frac{1}{N^2} \sum_{i, j} \sum_{\alpha, \beta} \omega_\alpha \omega_\beta \langle \sigma_i^{(1)} \sigma_j^{(1)} \rangle_\alpha \langle \sigma_i^{(2)} \sigma_j^{(2)} \rangle_\beta \\ &\approx \frac{1}{N^2} \sum_{i, j} \sum_{\alpha, \beta} \omega_\alpha \omega_\beta \langle \sigma_i^{(1)} \rangle_\alpha \langle \sigma_j^{(1)} \rangle_\alpha \langle \sigma_i^{(2)} \rangle_\beta \langle \sigma_j^{(2)} \rangle_\beta , \end{aligned} \quad (33)$$

where we assumed that, since the states α and β are pure states, one has $\langle \sigma_i \sigma_j \rangle_\alpha \approx \langle \sigma_i \rangle_\alpha \langle \sigma_j \rangle_\alpha$ (We pretend that all points are far apart. This is clearly not correct for $i = j$ but the error is negligible for large N). Finally

$$\langle q^2 \rangle \approx \sum_{\alpha, \beta} \omega_\alpha \omega_\beta \mathcal{Q}_{\alpha, \beta}^2 . \quad (34)$$

In general one has, for any integer r ,

$$\langle q^r \rangle \approx \sum_{\alpha, \beta} \omega_\alpha \omega_\beta \mathcal{Q}_{\alpha, \beta}^r , \quad (35)$$

namely (still with disorder dependent ω_α 's and $\mathcal{Q}_{\alpha, \beta}$'s)

$$\langle \delta(q - \frac{1}{N} \sum_i \sigma_i^{(1)} \sigma_i^{(2)}) \rangle = \sum_{\alpha, \beta} \omega_\alpha \omega_\beta \delta(q - \mathcal{Q}_{\alpha, \beta}) . \quad (36)$$

This is a remarkable relation between a quantity relative to pure states and a quantity that is directly accessible, e.g. with Monte Carlo simulation. This relation is quite useful since there is no simple way to characterize pure states for spin glasses, in contrast to Ising ferromagnets where a pure state can be selected by simply applying an infinitesimal constant magnetic field of suitable sign.

2.2 Solution of the model

We look for the absolute minimum of $\mathcal{A}(\{q_{a,b}\})$, namely the lowest stable solution of $\partial\mathcal{A}/\partial q_{a,b} = 0$ for all $q_{a,b}$ with generic n . The solution is then to be analytically continued to the limit $n \rightarrow 0$. One proceeds heuristically by first making an ansatz for the matrix $q_{a,b}$ and generic n , involving a few parameters x_i and q_i . Very surprising at first sight, the correct saddle point solution is a maximum of \mathcal{A} with respect to the x_i 's and q_i 's (and not a minimum), and if several maxima are found, one should usually take the largest. Once a candidate solution is found, one should check that this solution is stable (that the Hessian has only nonnegative eigenvalues). If no satisfactory solution is found, one try a more general ansatz (This is indeed a heuristic procedure).

The simplest ansatz is the replica symmetric (RS) ansatz [2], namely all $q_{a,b} = q_0$, and accordingly $P(q) = \delta(q - q_0)$. This ansatz has a (ferromagnetic) solution in the whole $T > 0$ half-plane, with $q_0 = 0$ and zero magnetization for $H = 0$, and $q_0 > 0$ and nonzero magnetization for $H \neq 0$. At zero magnetic field and $T < 1$, this ansatz has another solution with $q_0 \neq 0$ that should in principle be selected since it has a higher free energy than the first solution. However detailed investigation [28] of the eigenvalues of the Hessian shows that neither solution is a maximum of the integrand in (16), and accordingly both should be rejected, when the absolute value of H is below the so called AT line that starts at some nonzero H at $T = 0$ and reaches the $H = 0$ axis at $T_c = 1$ (see Fig 1). In the rest of the half $T > 0$ plane, the paramagnetic RS solution is stable, which means heuristically that it is the correct solution.

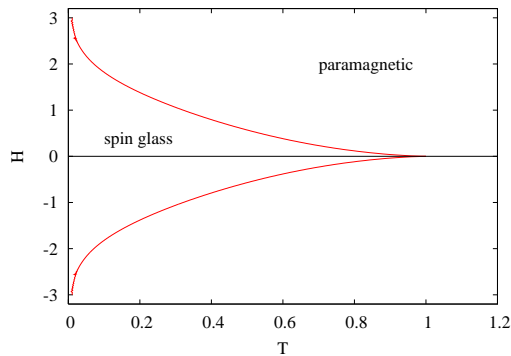


Fig. 1. Phase diagram of the SK model in the $T - H$ plane. The paramagnetic RS solution is valid outside of the area delimited by the AT lines and the H axis. The complementary region is the spin glass phase, where the ∞ -RSB ansatz gives the correct result.

One is thus led to a more general, non replica symmetric, ansatz. The correct (∞ -RSB) ansatz was found by Parisi [4, 7]. It is a hierarchical solution

that goes in an infinite number of steps. The first step is the so called “one step RSB ansatz”. The n replica are partitioned in n/x_1 blocks of x_1 replica. At this level, x_1 is an integer and x_1 divides n . One assumes that $q_{a,b} = q_1$ if a and b are in the same block, and that $q_{a,b} = q_0$ if they do not. With this rule we have $-\frac{n}{2}(1-x_1)$ elements $q_{\alpha,\beta}$ (for $a > b$) with value q_1 , and $-\frac{n}{2}(x_1-n)$ elements with value q_0 . If we plug this information into (29), and do formally the limit $n \rightarrow 0$, this gives

$$P(q) = x_1 \delta(q - q_0) + (1 - x_1) \delta(q - q_1), \quad (37)$$

which means that $P(q)$ has two peaks of weights x_1 and $1 - x_1$ respectively. Clearly this result only makes sense if $x_1 \in [0, 1]$. We started with a $n \times n$ matrix subdivided in $x_1 \times x_1$ blocks, and then let $n \rightarrow 0$. We have to admit that in this strange limit, the integer x_1 became a real variable $\in [0, 1]$.

In the next step, the so called “two steps RSB ansatz”, each diagonal block of size x_1 is divided in x_1/x_2 sub blocks of size x_2 and one assumes that now $q_{\alpha,\beta} = q_2$ in the diagonal sub-blocks, and is unchanged elsewhere.

Performing this procedure k times, we introduce a subdivision $n = x_0 > x_1 > x_2 > \dots > x_{k+1} = 1$, with integer x_0, x_1, \dots, x_k , $x_0/x_1, x_1/x_2, \dots, x_{k-1}/x_k$ and to a set of values for the overlaps q_0, q_1, \dots, q_k . Then

$$P(q) = \sum_{i=0}^k (x_{i+1} - x_i) \delta(q - q_i). \quad (38)$$

In order for this formula to makes sense, we have to assume that in the $n \rightarrow 0$ limit, the x_i variables became $0 = x_0 < x_1 < x_2 < \dots < x_{k+1} = 1$. Assuming now that the q_i 's form an increasing sequence, one has

$$\int_0^{q_m} P(q) dq = \sum_{i=0}^m (x_{i+1} - x_i) = x_{m+1} \quad m = 0, 1, \dots, k. \quad (39)$$

In the $k \rightarrow \infty$ limit, assuming that the increasing sequence q_i 's converges to a continuous function $q(x)$, with an inverse $x(q)$, this equation becomes

$$\int_0^q P(q') dq' = x(q), \quad P(q) = \frac{dx}{dq}. \quad (40)$$

We have similarly the equation, for any integer r ,

$$-\frac{2}{n} \sum_{a \neq b} q_{a,b}^r = \sum_{i=0}^k (x_{i+1} - x_i) q_i^r \sim \int_0^1 dx q(x)^r. \quad (41)$$

Finally $\mathcal{A}(q(x))$ is expressed as a (complicate) functional of $q(x)$, that should be maximized with respect to variations of the function $q(x)$ in order to give the free energy $f(T)$:

$$-f(T) = \frac{\beta}{4} \left(1 - 2q(1) + \int_0^1 dx q^2(x) \right) + \int_{-\infty}^{+\infty} \frac{dy}{\sqrt{2\pi q(0)}} \exp\left(-\frac{(y-H)^2}{2q(0)}\right) \phi(0, y), \quad (42)$$

where $\phi(0, y)$ is the solution, evaluated at $x = 0$, of the equation

$$\partial_x \phi(x, y) = -\frac{\partial_x q(x)}{2} \left[\partial_y^2 \phi(x, y) + \beta x (\partial_y \phi(x, y))^2 \right], \quad (43)$$

with the boundary condition

$$\phi(1, y) = \beta^{-1} \log(2 \cosh \beta y). \quad (44)$$

One can show [29] that the (∞ -RSB) solution is stable in the whole region where the paramagnetic RS solution is unstable. This means (heuristically) that we have found the correct solution for all H and $T > 0$. There is however no known close form solution neither for $q(x)$ ¹¹ nor for the corresponding free energy $f(T)$, and most articles in the literature use approximate estimates of $q(x)$, usually based on the truncated Hamiltonian (see next section), valid for $T \approx T_c$. Precise estimates can be obtained however either by an expansion of the functional in powers of $T_c - T$, or by numerical methods (see [30] for recent very precise estimates in the $H = 0$ case, and [31] in the $H \neq 0$ case).

For $H \neq 0$, the continuous non decreasing function $q(x)$ behaves as follows (see Fig 2): There exist values $0 \leq x_{min} \leq x_{max} \leq 1$ such that $q(x) = q_{min} \geq 0$ for $x \in [0, x_{min}]$, $q(x)$ increases for $x \in [x_{min}, x_{max}]$, and $q(x) = q_{max}$ for $x \in [x_{max}, 1]$. Accordingly the function $P(q)$ has two delta function peaks located at $q(x) = q_{min}$ and $q(x) = q_{max}$ respectively, and is nonzero between. The transition on the AT line is continuous, with $q_{min} \rightarrow q_{max}$, as the AT lined is approached.

The value q_{max} is interpreted as q_{EA} , the overlap between two configurations in the same pure state

$$q_{EA} = \frac{1}{N} \sum_i \langle \sigma_i \rangle_\alpha \langle \sigma_i \rangle_\alpha. \quad (45)$$

One can show that q_{EA} is independent of α . This definition is in agreement with the one given in the introduction (2) thanks to the wide separation of time scales in the model: A given configuration stays a very long time in the same pure state, and accordingly the correlation function $C(t)$ has a plateau of height q_{EA} .

As $H \rightarrow 0$, $q_{min} \rightarrow 0$ and the corresponding peak disappears. When H is exactly zero, $P(q)$ which is nonzero for $0 < q_{min} \leq q \leq q_{max}$ for $H \neq 0$ becomes symmetric (obviously the two limits $N \rightarrow \infty$ and $H \rightarrow 0$ do not commute). At $H = 0$, $P(q)$ is made of two delta peaks located at $\pm q_{max} = \pm q_{EA}$ with a continuum between. As shown in [30], and in contradiction with many drawings in the literature (and Fig 3), $P(q)$ has a minimum at a nonzero

¹¹ From now on, $q(x)$ denotes the solution of the saddle point equations $q^{SP}(x)$.

value of q (at least as soon as $T < 0.96 \dots$) and behaves like $a + bq^2 + c|q|^3 + \dots$, with $c \neq 0$ for small q . When $T \rightarrow T_c$, $q_{EA} \rightarrow 0$, namely the transition is continuous.

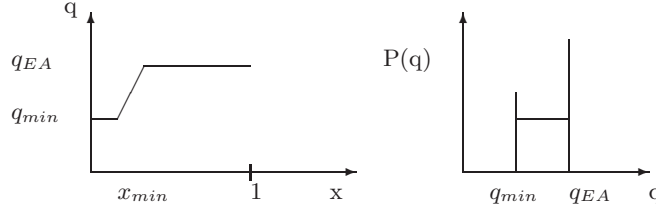


Fig. 2. Schematic representation of the ∞ -RSB solution for $H \neq 0$: $q(x)$ as a function of x and $P(q)$ as a function of q , with $q_{EA} = q_{max}$. In the actual solution the increasing portion of $q(x)$ and the corresponding continuum in $P(q)$ are not straight.

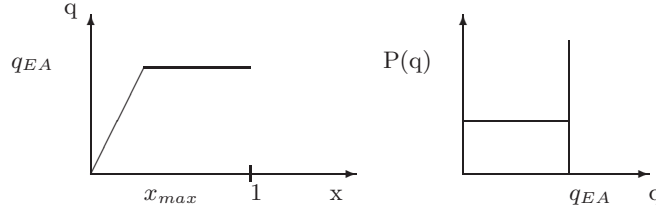


Fig. 3. Schematic representation of the ∞ -RSB solution for $H = 0$: $q(x)$ as a function of x and $P(q)$ as a function of q , with $q_{EA} = q_{max}$. In the actual solution the increasing portion of $q(x)$ and the corresponding continuum in $P(q)$ are not straight. In this $H = 0$ case, $P(q)$ is symmetric in q . Only the $q > 0$ part of $P(q)$ is represented here.

2.3 Properties of the solution

Among the fascinating features of Parisi solution, is ultrametricity [32]. Taking three clones, one can show that

$$\begin{aligned}
P(q_{1,2}, q_{2,3}, q_{3,1}) &= \langle \delta(q_{1,2} - \sum_{i=1}^N \sigma_i^{(1)} \sigma_i^{(2)}) \delta(q_{2,3} - \sum_{i=1}^N \sigma_i^{(2)} \sigma_i^{(3)}) \delta(q_{3,1} - \sum_{i=1}^N \sigma_i^{(3)} \sigma_i^{(1)}) \rangle \\
&= \frac{1}{n(n-1)(n-2)} \sum_{a,b,c}^{a \neq b, b \neq c, c \neq a} \delta(q_{1,2} - q_{a,b}) \delta(q_{2,3} - q_{b,c}) \delta(q_{3,1} - q_{c,a}) .
\end{aligned} \tag{46}$$

The ∞ -RSB solution for the $q_{a,b}$'s has the property that this probability is zero unless the three overlaps $q_{1,2}, q_{2,3}, q_{3,1}$ satisfy the ultrametricity constraints: at least two overlaps are equal, and the third is smaller or equal to their common value. Ultrametricity generalizes to pure states, where one defines a distance between pure states α and β , as

$$\begin{aligned}
d_{\alpha,\beta} &= \frac{1}{N} \sum_i (\langle \sigma_i \rangle_\alpha - \langle \sigma_i \rangle_\beta)^2, \\
&= \mathcal{Q}_{\alpha,\alpha} + \mathcal{Q}_{\beta,\beta} - 2\mathcal{Q}_{\alpha,\beta} = 2(q_{EA} - \mathcal{Q}_{\alpha,\beta}),
\end{aligned} \tag{47}$$

since all self overlaps are equal to q_{EA} .

Another feature [32] of the Parisi solution is that some intensive observables are not self averaging¹² namely some thermodynamic averages $\langle A \rangle$ retain a (disorder) sample dependence even in the large N limit, i.e. $\lim_{N \rightarrow \infty} (\overline{\langle A \rangle^2} - \langle \overline{A} \rangle^2) \neq 0$. Among self averaging quantities are the internal energy, the free energy, the magnetization and the Edwards–Anderson order parameter q_{EA} . The order parameter distribution function $P_J(q)$ is an example of a non self averaging, quantity. The general rule is that observables that do not involve correlations between different pure states are self averaging, those that involve such correlations are not self averaging.

In order to show that the order parameter distribution function $P_J(q)$ is not self averaging, one considers four clones, and the probability $P_J(q_{1,2}, q_{3,4})$. Clearly $P_J(q_{1,2}, q_{3,4}) = P_J(q_{1,2})P_J(q_{3,4})$, since clones are non interacting. However, we will show that

$$\overline{P_J(q_{1,2})P_J(q_{3,4})} \neq \overline{P_J(q_{1,2})} \overline{P_J(q_{3,4})}, \tag{48}$$

which implies that $P_J(q)$ is not self averaging, since a self averaging $P_J(q)$ would not depend on J for a large system. The evaluation of $\overline{P_J(q_{1,2}, q_{3,4})}$ is done by considering moments of the distribution

¹² For a discussion of non-self averaging in other random systems, see [33].

$$\begin{aligned} & \int dq_{1,2} q_{1,2}^r \int dq_{3,4} q_{3,4}^s \overline{P_J(q_{1,2})P_J(q_{3,4})} = \overline{\langle q_{1,2}^r q_{3,4}^s \rangle} \quad (49) \\ & = \frac{1}{n(n-1)(n-2)(n-3)} \sum_{\substack{a,b,c,d \\ \text{all different}}} q_{a,b}^r q_{c,d}^s, \end{aligned}$$

with integer r and s .

We now use the very powerful property of replica equivalence, namely the observation that in Parisi solution one has:

$$\sum_b q_{a,b} \quad \text{independent of } a. \quad (50)$$

In order to use this property, one notes that .

$$\begin{aligned} \sum_{\substack{a,b,c,d \\ \text{all different}}} q_{a,b}^r q_{c,d}^s &= \sum_{a,b} \sum_{c,d} q_{a,b}^r q_{c,d}^s - 4 \sum_{a,b,d} q_{a,b}^r q_{a,d}^s \\ &+ 2 \sum_{a,b} q_{a,b}^r q_{a,b}^s. \end{aligned} \quad (51)$$

Since the sum $\sum_{a,b,d} q_{a,b}^r q_{a,d}^s$ is unrestricted, one can write it as

$$\sum_{a,b} q_{a,b}^r \sum_d q_{a,d}^s = \sum_{a,b} q_{a,b}^r \frac{1}{n} \sum_{c,d} q_{c,d}^s. \quad (52)$$

In the $n \rightarrow 0$ limit, one obtains

$$\overline{\langle q_{1,2}^r q_{3,4}^s \rangle} = \frac{1}{3} \overline{\langle q_{1,2}^{r+s} \rangle} + \frac{2}{3} \overline{\langle q_{1,2}^r \rangle} \overline{\langle q_{3,4}^s \rangle}, \quad (53)$$

$$\overline{P_J(q_{1,2})P_J(q_{3,4})} = \frac{1}{3} \overline{P_J(q_{1,2})} \delta(q_{1,2} - q_{3,4}) + \frac{2}{3} \overline{P_J(q_{1,2})} \overline{P_J(q_{3,4})}, \quad (54)$$

in agreement with (48). It is interesting that the above relation can be proven rigorously [34] (the proof given in this paper is for the $r = s = 2$ case).

The method used by Parisi to solve the SK model is far from mathematical rigor, to say the less, and it took time to convince the skeptics that it does give the correct result. Very recently however beautifully rigorous results have been obtained. One is a rigorous proof [35] that the free energy density of the SK model has a well defined limit as $N \rightarrow \infty$, a long awaited result that is far from trivial for a disordered model with infinite connectivity. Then the method was extended to show that the free energy of the Parisi solution is a lower bound on the free energy of the model [36], and finally to prove that it is equal to the free energy of the model [37]. More recently a proof appeared that the AT line is indeed the boundary of the paramagnetic replica symmetric region [38].

2.4 Critical exponents

At zero magnetic field, the transition at T_c is of second order and one can define critical exponents. The order parameter is the mean overlap $\overline{\langle q \rangle}$, and one has

$$\begin{aligned} \overline{\langle q \rangle} &\propto (T_c - T)^\beta & T < T_c & \quad \text{with} \quad \beta = 1, & (55) \\ &= 0 & T > T_c, & \\ \chi_{SG} &= N \overline{\langle q^2 \rangle}, \\ &\propto (T_c - T)^{-\gamma} & T > T_c & \quad \text{with} \quad \gamma = 1, \\ &= \infty & T < T_c. & \end{aligned}$$

The values of the critical exponents are $\alpha = -1$ (the specific heat has a cusp at the critical temperature), $\beta = 1$, $\eta = 0$ (the mean field value), $\gamma = 1$, and $\nu = 1/2$. Hyper scaling holds provided one uses the value $d = 6$ of the space dimension in the formula. This is related to the fact that $d = 6$ is the upper critical dimension of the replica field theory.

2.5 The truncated model

We have seen that for $H = 0$ the high T solution has $q_{a,b} = 0 \forall a, b$. It is accordingly natural to expand \mathcal{A} in powers of $q_{a,b}$ in (16). Only the terms up to the order four are usually kept, as one can show that this gives the correct critical behavior and the correct qualitative description of the low T phase. This truncated model has been very useful historically. It is also quite useful in order to study finite size effects (See Subsec. 4.1).

The trace over the spins is straightforward. For a given replica index, the trace is equal to zero for an odd power of the replicated spins and to two for an even power. Neglecting powers of $q_{a,b}$ higher than four, one obtains the truncated model (written for $H = 0$):

$$\beta f_N = -\ln 2 - \frac{\beta^2}{4} - \lim_{n \rightarrow 0} \frac{1}{nN} \ln \int \left[\prod_{a < b} \sqrt{\frac{N}{2\pi\beta^2}} d\tilde{q}_{ab} \right] \exp(-N\beta\mathcal{L}[\tilde{q}]). \quad (56)$$

$$\begin{aligned} \beta\mathcal{L}[\tilde{q}] &= \frac{\tau}{2} \sum_{a,b} \tilde{q}_{a,b}^2 - \frac{1}{6} \sum_{a,b,c} \tilde{q}_{a,b} \tilde{q}_{b,c} \tilde{q}_{c,a} & (57) \\ &- \frac{1}{8} \sum_{a,b,c,d} \tilde{q}_{a,b} \tilde{q}_{b,c} \tilde{q}_{c,d} \tilde{q}_{d,a} + \frac{1}{4} \sum_{a,b,c} \tilde{q}_{a,b}^2 \tilde{q}_{a,c}^2 - \frac{1}{12} \sum_{a,b} \tilde{q}_{a,b}^4 + \dots, \end{aligned}$$

where $\tau = (T^2 - 1)/2$. We use the notation $\tilde{q} = q\beta^2 = q/T^2$ in order to simplify the formula, and write unrestricted sums over the replica indexes,

considering $\{q_{a,b}\}$ as a symmetric matrix with zero elements on the diagonal. For $T > T_c$, $\tau > 0$ and the paramagnetic solution is stable as it should.

A further simplification, that leads to simpler analytical computations, has been proposed by Parisi in one of his seminal articles [6]. It amounts to replace (57) by

$$\beta\mathcal{L}[\tilde{q}] = \frac{\tau}{2} \sum_{a,b} \tilde{q}_{a,b}^2 - \frac{1}{6} \sum_{a,b,c} \tilde{q}_{a,b} \tilde{q}_{b,c} \tilde{q}_{c,a} - \frac{y}{8} \sum_{a,b} \tilde{q}_{a,b}^4, \quad (58)$$

keeping the only fourth order term that is responsible for the replica symmetry breaking and using the value $y = 2/3$. This is the Parisi approximation of the truncated model, sometimes called the truncated model, sometimes the reduced model. In most cases this approximation has only mild effects, changing the numerical value of some coefficients. In a few cases however, it gives qualitatively wrong results.

2.6 Some variant of the model

Two variants of the Sherrington–Kirkpatrick model are worth mentioning. The first is the spherical Sherrington–Kirkpatrick model, defined by the same Hamiltonian (1) as the original model, but with continuous spins σ_i obeying the spherical constraint

$$\sum_i \sigma_i^2 = N. \quad (59)$$

It can be exactly solved [39] in the thermodynamic limit without the use of replica. It can also be solved using the replica trick, and both methods give the same results. The physics of the spherical model is however quite different from the one of the original model: It is paramagnetic for all $T \geq 0$ and $H \neq 0$ but for the region $H = 0$ and $T \leq 1$, where the RS ansatz with nonzero q_0 gives the correct solution. On the other hand, much has been learned of the dynamics of spin glass models from analytical studies of the spherical SK model (see e.g. [23]).

The second variant is the p -spin model [40], where all combinations of p spins are coupled together, with the Hamiltonian

$$H = - \sum_{1 \leq i_1 < i_2 < \dots < i_p \leq N} J_{i_1, \dots, i_p} \sigma_{i_1} \dots \sigma_{i_p} - H \sum_{i=1}^N \sigma_i, \quad (60)$$

where the J_{i_1, \dots, i_p} 's are quenched independent identically distributed random variables with zero mean and square deviation $\overline{J^2} = \frac{p!}{2N^{p-1}}$. The spins are Ising spins $\sigma_i = \pm 1$. The original SK model is recovered for $p = 2$. The $p \geq 3$ p -spin model has a very different physics than the SK model: in the $H = 0$ case,

by decreasing the temperature from $T = \infty$ one encounters three successive phase transitions, a purely dynamical transition, then a transition to a state with one-step RSB, and finally a transition to a state with ∞ -RSB. For details seen [40, 41]. One can define a spherical p-spin model with continuous spin variables obeying the spherical constraint [42, 43]. Many analytical results have been obtained for the later model. Some subtle qualitative differences are found however between the original and spherical p-spin models [41].

3 Simulations techniques

Spin glass simulations are very difficult, since on the one hand the dynamics is very slow, and on the other hand one needs to perform the simulation for many disorder samples. Both effects are stronger and stronger as T decreases and/or N increases. The SK model is no exception. It is furthermore much harder to simulate than finite dimension spin glass models since one needs $O(N)$ operations to update one spin variable, and not $O(1)$. The p-spins model is even harder with $O(N^{p-1})$ operations to update a single spin. For a simulation of the $p = 3$ p-spin model, see [44].

The best existing algorithm is called under various names such as “Replica Monte Carlo”, “Exchange Monte Carlo” and “Parallel Tempering” [45]. This algorithm is well known and consists in simulating n_{PT} clones of the system in parallel at temperatures $T_1 < T_2 < \dots < T_{n_{PT}}$ respectively. Two kind of Monte Carlo moves are performed

- Step 1 (the parallel Metropolis step): Metropolis update of each clone independently.
- Step 2 (the exchange step): Conditionally exchange of the spin configurations of all pairs of clones, with a suitable acceptance probability.

In both steps the acceptance probability is the usual Metropolis acceptance probability. If π_x is the Boltzmann weight of state x , with energy E_x , namely $\pi_x = \exp(-E_x/T) / \sum_y \exp(-E_y/T)$, and $p_{x,y}$ the probability to go from state x at time t to state y at time $t + 1$, one desires to fulfill the condition

$$\sum_x \pi_x p_{x,y} = \pi_y . \quad (61)$$

This condition is called balance (stationarity in the mathematical literature). Together with ergodicity (irreducibility in the mathematical literature) and the more technical condition of aperiodicity, this ensures that the Markov chains converges towards the Boltzmann distribution [46, 47, 48].

Balance is obtained by requiring that the probability to propose the move $p_{x,y}^{(0)}$ and the probability to accept it $a_{x,y}$ satisfy ¹³ (One has clearly $p_{x,y} = p_{x,y}^{(0)} a_{x,y}$)

¹³ I consider the general case $p_{x,y}^{(0)} \neq p_{y,x}^{(0)}$, even if the equality usually holds.

$$\frac{p_{x,y}^{(0)} a_{x,y}}{p_{y,x}^{(0)} a_{y,x}} = \min(1, \exp(-1/T(E_x - E_y))) . \quad (62)$$

A common misconception is that after the exchange step the system is not at equilibrium, and that this introduces a bias, that one may minimize by making many parallel Metropolis steps (step 1) between each exchange step. This is not correct, balance is enough to ensure convergence towards the Boltzmann weight.

There is a considerable freedom in implementing this algorithm. The parallel Metropolis step is usually done by updating all spins, either systematically (all spins are updated one after the other), or randomly (choose one spin at random, then update it, then choose another, ...). The exchange step is usually restricted to the $n_{PT} - 1$ pairs of clones with neighboring temperatures (the acceptance rate of this exchange is higher), and can be done systematically (update the pair at temperatures T_1 and T_2 , then the pair at temperatures T_2 and T_3 , ...) or randomly. Step two clearly takes no time as compared to step one. One usually alternates the two steps, one parallel tempering step (PT step) consists accordingly of one parallel Metropolis step followed by one exchange step.

The choice of the sequence $T_1 < T_2 < \dots < T_{n_{PT}}$ leads also to considerable freedom. One constraint is that the acceptance rate of the chain exchange (chain of energy E at temperature T with chain of energy E' at temperature T')

$$\begin{aligned} \frac{a_{T,T'}}{a_{T',T}} &= \min(1, \exp(-(E/T' + E'/T)) / \exp(-(E/T + E'/T'))) \quad (63) \\ &= \min(1 - \exp(-(E - E')(1/T - 1/T'))) , \end{aligned}$$

should not be too small. The acceptance rate is thus governed by the combination $(T' - T)^2 dE/dT$, with $dE_N/dT = N d e_N(T)/dT = N c_N(T)$, where $c_N(T)$ is the specific heat per spin, which is regular for all temperatures (and weakly N dependent) in the SK model. One may [49] adjust for every system size N the number n_{PT} and the values of the temperature of the clones in such a way that $(T_{i+1} - T_i)^2 N c_N(T)$, $i = 1, 2, \dots, n_{PT} - 1$ is roughly independent of i and N . There is however no guaranty that this choice is optimal, for example that it minimizes the statistical errors. A more satisfactory prescription is to maximize the number of tunnelings, namely the number of times a given clone goes from the minimal temperature to the maximal temperature (or the other way), as proposed recently in [50]. .

3.1 An example of Monte Carlo simulation

In what follows I will use data generated in collaboration with Enzo Marinari [9] for $H = 0$ (with $N = 64$ to 4096, $T \in [0.4, 1.325]$) and Barbara

Coluzzi [52] for $H \neq 0$ (for N up to 3200). For the purpose of these notes, I performed additional small simulations in order to measure the number of tunnelings as a function of N . I considered $N = 64, 256, \text{ and } 1024$. The temperatures of the clones are equidistant with $T = 0.4, 0.425, 0.45, \dots, 1.325$ (here $n_{PT} = 38$), with 128 disorder samples (16 for $N = 1024$), performing 400000 PT steps, starting from very well equilibrated configurations.

As shown in Fig. 4, the number of tunnelings is dramatically decreasing as N grows. Figure 4 gives another indicator of the algorithm behavior: the spread of the distribution of times spent by a given chain at each temperature. With infinite statistics, each chain should spend the same amount of time at each temperature. I have measured for each disorder sample the maximal (pop-max) and minimal (pop-min) time spent (in unit of PT steps) by each chain at each temperature. The average time (pop-avg) is equal to $400000/n_{PT} = 10526$. These numbers are plotted in Fig. 4 as a function of N . The situation is clearly degrading as N grows. Analyzing the $N = 4096$ data of [9] (The results of a massive numerical effort, with 520000 PT steps and $\Delta T = 0.0125$) one finds pop-min as low as 16.5.

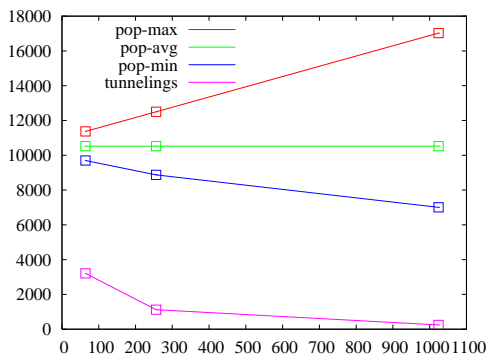


Fig. 4. From top to bottom: maximal (pop-max), average (pop-avg) and minimal (pop-min) times spent by a clone at a given temperature as a function of the number of sites. Lines have been drawn between the points to guide the eyes. The line in the bottom is the average number of tunnelings.

3.2 Comparison with theoretical expectations

Figure 5 shows $P_J(q)$ for eight different disorder realizations, using the data of [9]. Here $N = 4096$ and $T = 0.4$, a pair of values that is at the borderline of what can be done with current algorithms and computer resources. We are well inside the spin-glass phase, and the number of spins is equal to the number of spins of a 16^3 lattice ¹⁴. These eight samples are just the eight first

¹⁴ This is to say that it is a large system, by current spin glass standards.

samples generated by our computer program, they have not been selected afterwards. One sees clearly that the shape of $P_J(q)$ is strongly fluctuating from sample to sample. In view of (36) this is very suggestive of the existence of several (disorder dependent) pure states. The two extreme peaks correspond to the self overlap q_{EA} (which is the same for all pure states), the other peaks correspond to cross overlaps. If the shape of $P_J(q)$ is strongly fluctuating, the position of the outmost peak is not, in agreement with the prediction that q_{EA} is self-averaging. One notes finally that the curves are reasonably symmetric, this is a very strong sign that the Monte Carlo statistics is sufficient.

The non self averaging of $P_J(q)$ makes the measurement of the disorder averaged $P(q)$ quite difficult on large lattices. This is exemplified in Fig. 6, which presents our estimate of this average with all 256 disorder samples. The wiggles are artifacts due to the finite number of samples.

The Parisi solution has the quite unusual prediction that the low temperature phase extends to nonzero H (up to the AT line). This prediction is unfortunately hard to check numerically, as can be seen in Fig. 7 from [52]. Even the very existence of a peak at q_{min} is not clear from the data. In order to see this peak unambiguously, one would need to satisfy two conflicting constraints, H should not be too small, since the weight of the peak goes to zero as $H \rightarrow 0$. It should also not be too close to the AT line since $q_{min} \rightarrow q_{max}$ in this limit. Clearly much larger systems would be needed in order to see a clear distinct peak at q_{min} .

A classical method to locate the critical point from numerical data uses the Binder parameter (the Kurtosis of the order parameter distribution function). For the SK model this is

$$B_N(H, T) = \frac{1}{2} \left(3 - \frac{\overline{\langle (q - \langle q \rangle)^4 \rangle}}{\overline{\langle (q - \langle q \rangle)^2 \rangle}^2} \right). \quad (64)$$

Here $B(H, T)$ is defined ¹⁵ in such a way that it is zero if $P_J(q)$ is Gaussian (namely at high enough temperature) and one for a two equal weight delta functions distribution. In finite dimension we know from finite size scaling that $B_N(H, T)$ is a function of $(T - T_c(H))L^{1/\nu} = (T - T_c(H))N^{1/(\nu d)}$, and accordingly the curves for $B_N(H, T)$ drawn for different values of N should all cross at the critical point $T_c(H)$. This provides a very convenient numerical method to determine a critical point. In the SK model, finite size scaling holds with $d = 6$ and $\nu = 1/2$ (see Subsec. 2.4). The Binder parameter method to locate T_c works nicely at zero magnetic field, the curves for different values of N decrease monotonously as a function of T , are well separated away from T_c and cross nicely at T_c . This is not the case at nonzero magnetic field [52], at least with system sizes one can currently simulate.

It is fair to admit that, from a numerical perspective, the AT line remains elusive. This is not a problem in the SK model case since there is no doubt

¹⁵ When $H = 0 < q \rangle = 0$, and the formula simplifies substantially.

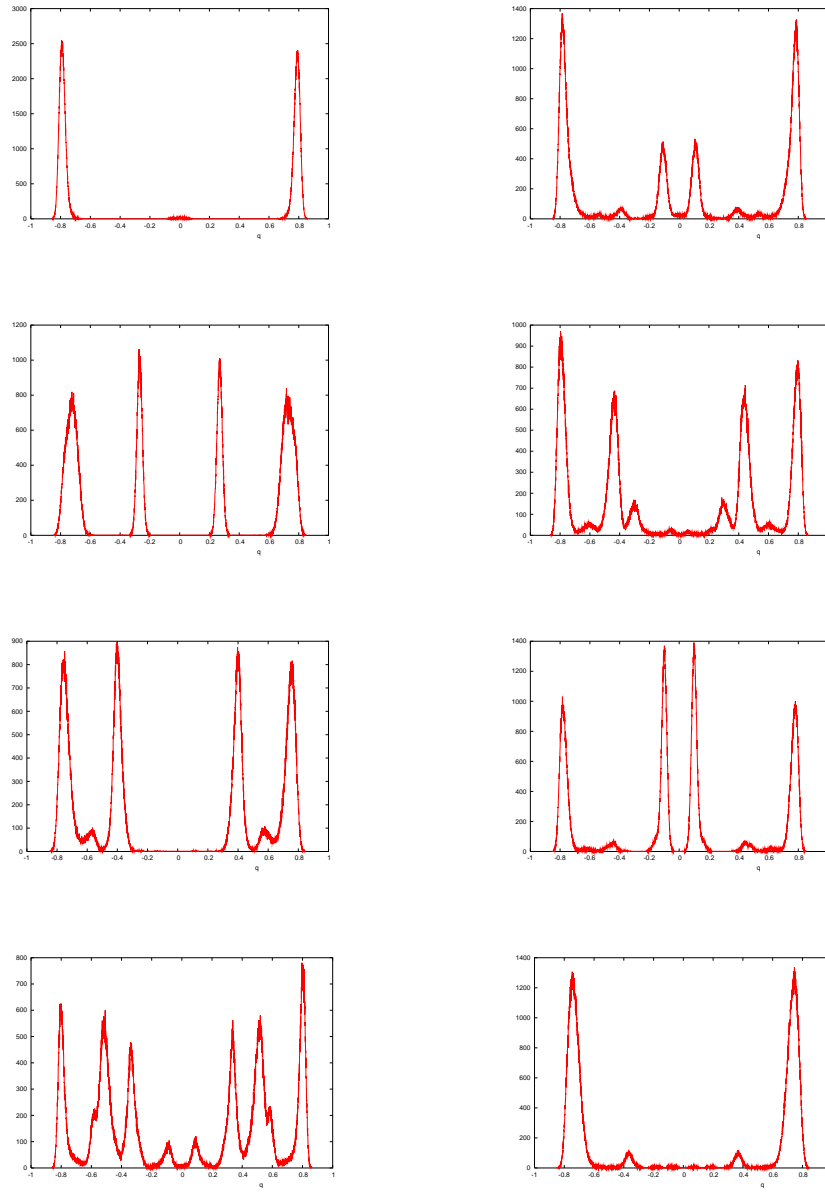


Fig. 5. $P_J(q)$ for eight different disorder realization. Here $N = 4096$ and $T = 0.4$

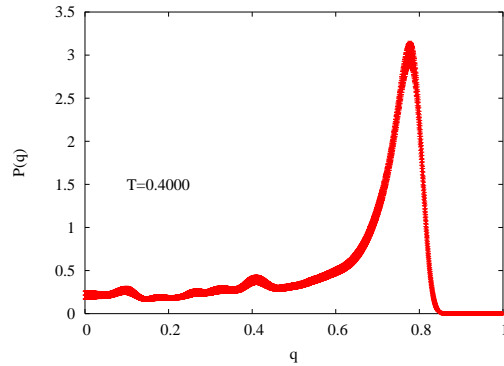


Fig. 6. The disorder averaged $P(q)$ for $q > 0$ and zero magnetic field. Here $N = 4096$ and $T = 0.4$. The wiggles are a fluctuation due to the finite (256) number of disorder samples. For this value of T , the infinite volume limit of q_{EA} is [51] $q_{EA} = 0.759$.

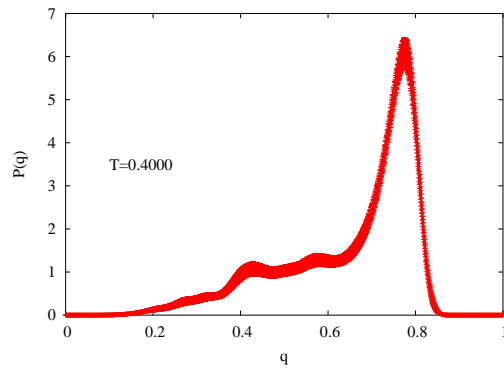


Fig. 7. The disorder averaged $P(q)$ for $q > 0$ at nonzero $H = 0.3$. Here $N = 3200$ and $T = 0.4$. For these values of H and T , the infinite volume limit of q_{EA} and q_{min} are [51] $q_{EA} = 0.759$ and $q_{min} \approx 0.44$. The self-overlap q_{EA} is nearly H independent at fixed T . This is a consequence of the so called Parisi–Toulouse hypothesis .

about the existence and exact location of this transition line. It become annoying however if one has the EAI case in mind.

I will close this section by mentioning that there are some numerical evidences for ultrametricity, in the sense that triplets of typical spin configurations (with the same disorder configuration) $\{\sigma_i^{(1)}\}, \{\sigma_i^{(2)}\}, \{\sigma_i^{(3)}\}$ do fulfill [53] the ultrametric constraint. There is however no numerical evidences [54] for the full treelike structure of states, as predicted by Parisi solution.

4 Finite size effects for the free energy and the internal energy

Numerical simulations are obviously limited to finite systems, and simulations of spin glasses are indeed limited to very small systems. A detailed understanding of finite size effects in spin glass models is accordingly highly desirable. In what follows, I will only consider the free energy and the internal energy at zero magnetic field. I define the exponents μ and ω according to the equations

$$\begin{aligned} f_N(T) &= f(T) + B(T)N^{-\mu} + \dots \\ e_N(T) &= e(T) + C(T)N^{-\omega} + \dots, \end{aligned} \quad (65)$$

where $f(T)$ and $e(T)$ are the infinite volume free energy and internal energy at temperature T .

4.1 Paramagnetic phase

In the high temperature phase, the finite size effects for the internal energy and free energy can be obtained from the truncated model of (56,57). At first order, one keeps only the quadratic term in $\mathcal{L}[\tilde{q}]$, with the result

$$\begin{aligned} \beta f_N(T) &= -\ln 2 - \frac{\beta^2}{4} - \lim_{n \rightarrow 0} \frac{1}{nN} \ln \int \left[\prod_{a < b} \sqrt{\frac{N}{2\pi\beta^2}} d\tilde{q}_{ab} \right] \exp(-N\tau \sum_{a < b} q_{a,b}^2) \\ &= -\ln 2 - \frac{\beta^2}{4} - \lim_{n \rightarrow 0} \frac{1}{nN} \ln \left[\prod_{a < b} \sqrt{\frac{1}{2\tau\beta^2}} \right] \end{aligned} \quad (66)$$

$$= -\ln 2 - \frac{\beta^2}{4} - \frac{1}{4N} \ln 2\tau\beta^2. \quad (67)$$

The neglected terms in $\mathcal{L}[\tilde{q}]$ can be included by expanding the exponent as a power series [55, 56, 57]. Each term is represented by a graph without external leg. Each line gives a factor $1/(N\tau)$, and each vertex a factor N . Introducing the number of lines $\#L$, of vertices $\#V$ and loops $\#B$ of a given graph, one finds that the graph behaves like $N^{\#V-1}(N\tau)^{-\#L} = N^{-\#B}\tau^{-\#L}$. Organizing the expansion as a loop expansion, one obtains an expansion in powers of $1/N$, with the most singular term (as $\tau \rightarrow 0$) at each order, given by the contribution of the cubic term in \mathcal{L} (for which $\#L = 3(\#B - 1)$). The development up to the $O(1/N^4)$ order (four loops) has been obtained in [55] (the terms of order $1/N^4$ are not given in the paper, but have been used in the re-summation at T_c). Results up to five loops, for arbitrary n but omitting the quartic terms in \mathcal{L} can be found in [57].

The internal energy is simply obtained through the equation

$$e_N(T) = \frac{d}{d\beta} f_N(T), \quad (68)$$

that holds also at finite N .

As one approaches the critical point both expansions for $f_N(T)$ and $e_N(T)$ become singular, and need to be re-summed. Writing symbolically the N dependent part of $f_N(T \approx T_c)$ as

$$\begin{aligned} & - \lim_{n \rightarrow 0} \frac{1}{nN} \ln \int \left[\prod_{a < b} \sqrt{\frac{N}{2\pi}} d\tilde{q}_{ab} \right] \exp(-N(\tau Q^2 + Q^3 + Q^4)) \\ & = - \lim_{n \rightarrow 0} \frac{1}{nN} \ln \int \left[\prod_{a < b} \sqrt{\frac{(xN)^{1/3}}{2\pi}} d\tilde{q}_{ab} \right] \exp(-(Q^2 + x^{1/2}Q^3 + x^{2/3}/N^{1/3}Q^4)), \end{aligned} \quad (69)$$

where $x = 1/(N\tau^3)$, we obtain the N dependent part of $f_N(T_c)$ as the $x \rightarrow \infty$ limit of

$$\frac{\ln N}{12N} - \frac{1}{N} \lim_{n \rightarrow 0} \frac{1}{n} \ln \int \left[\prod_{a < b} \sqrt{\frac{x^{1/3}}{2\pi}} d\tilde{q}_{ab} \right] \exp(-(Q^2 + x^{1/2}Q^3 + x^{2/3}/N^{1/3}Q^4)).$$

Treating the order four term as a perturbation one obtain finally

$$f_N(T_c) = -\ln 2 - 1/4 + \frac{\ln N}{12N} + \frac{f_{(-1)}}{N} + \frac{f_{(-4/3)}}{N^{4/3}} + \dots, \quad (70)$$

$$e_N(T_c) = -\frac{1}{2} + \frac{e_{(-2/3)}}{N^{2/3}} + O(N^{-1}). \quad (71)$$

The behavior of the internal energy is the one expected from scaling. At a critical point, the singular part of the internal energy for a L^d system behaves¹⁶ like $L^{1/\nu-d}$. Using the values $\nu = 1/2$ and $d = 6$ (see Subsec. 2.4) one finds that the singular part of the internal energy does behave like $N^{-2/3}$. In order to obtain the values of the coefficients $f_{(-1)}$, and $e_{(-2/3)}$, one needs to handle the theory in the strong coupling $x \rightarrow \infty$ regime. This is not easy and these values are poorly determined [55].

4.2 Zero temperature

With the discovery of very efficient algorithms for determining the ground state of a spin glass finite system (at fixed \mathcal{J}), the physics of zero temperature spin glass has blossomed in the recent years. This includes detailed studies of the finite size effects of the internal energy. In the specific case of the SK model, good evidences have been obtained for a $1/N^{2/3}$ behavior for the internal energy for both Gaussian and binary disorder distributions [58, 59, 60, 61, 62, 63], as summarized in Tab. 1. The value $\omega = 2/3$ is exact for the spherical Sherrington–Kirkpatrick model [64].

¹⁶ This follows from the scaling expression $f = 1/L^d \tilde{F}((T - T_c)L^{1/\nu})$.

	$P(\mathcal{J})$	N_{max}	ω
Palassini [59]	Gaussian	199	0.673 ± 0.002
Bouchaud et al [60]	± 1	300	0.66 ± 0.02
Boettcher [61]	± 1	1023	0.672 ± 0.005
Katzgraber et al [62]	Gaussian	192	0.64 ± 0.01
Pal [63]	both	2048	$\approx 2/3$

Table 1. Numerical estimates for the exponent ω at $T = 0$ for the Sherrington–Kirkpatrick model: reference, disorder distribution, maximum system size and result.

4.3 Using the Guerra and Toninelli formalism

As shown in [65], one can use the so called Guerra and Toninelli interpolation formalism, an ingredient in the proof [35] that the free density energy of the Sherrington–Kirkpatrick model converges in the infinite volume limit N , as the basis of a powerful numerical method to compute the finite size corrections to the free energy of the model. Guerra and Toninelli introduced the partition function

$$\begin{aligned}
Z_N(t) = \sum_{\{\sigma\}} \exp & \left(\beta \left(\sqrt{\frac{t}{N}} \sum_{1 \leq i < j \leq N} J_{ij} \sigma_i \sigma_j \right. \right. \\
& + \sqrt{\frac{1-t}{N/2}} \sum_{1 \leq i < j \leq N/2} J'_{ij} \sigma_i \sigma_j \\
& \left. \left. + \sqrt{\frac{1-t}{N/2}} \sum_{N/2 < i < j \leq N} J''_{ij} \sigma_i \sigma_j \right) \right) \exp(\beta H \sum_i \sigma_i), \tag{72}
\end{aligned}$$

that involves a parameter t that interpolates between the SK model with N sites ($t = 1$) and a system of two un-coupled SK models with $N/2$ sites ($t = 0$). The $J_{i,j}$'s, $J'_{i,j}$'s and $J''_{i,j}$'s are independent identically distributed Gaussian random numbers. It is straightforward to show that

$$\begin{aligned}
\beta(f_N(T) - f_{N/2}(T)) &= \frac{\beta^2}{4} \int_0^1 dt \overline{\left\langle (q_{12})^2 - \frac{1}{2}(q_{12}^{(1)})^2 - \frac{1}{2}(q_{12}^{(2)})^2 \right\rangle} \tag{73} \\
&= \frac{\beta^2}{4} \int_0^1 dt \mathcal{D}(t) \quad \mathcal{D}(t) \leq 0,
\end{aligned}$$

where

$$\begin{aligned}
 q_{12} &= \frac{1}{N} \sum_{i=1}^N \sigma_i \tau_i, & q_{12}^{(1)} &= \frac{2}{N} \sum_{i=1}^{N/2} \sigma_i \tau_i, \\
 q_{12}^{(2)} &= \frac{2}{N} \sum_{i=N/2+1}^N \sigma_i \tau_i.
 \end{aligned}
 \tag{74}$$

In the above formulas, the σ_i 's and τ_i 's are the spins of two real replica, q_{12} is the usual overlap, for the N sites system, $q_{12}^{(1)}$ and $q_{12}^{(2)}$ are the overlaps restricted to the two subsystems with $N/2$ sites. The right hand side of (73) can be evaluated with Monte Carlo simulation. I use the Parallel Tempering algorithm, with $T \in [0.4, 1.3]$ and uniform $\Delta T = 0.025$. A total of $2 \cdot 10^5$ sweeps of the algorithm was used for every disorder sample. The quenched couplings have a binary distribution in order to speed up the computer program. Using the cumulant expansion (7) one can show that in the paramagnetic phase, the replacement of Gaussian couplings by binary couplings induces a leading $1/N$ correction to the free energy density, of the same order as the leading finite size correction (see below). One can argue that the effect of the binary couplings is also $1/N$ in the spin glass phase, and is thus negligible with respect to the leading $1/N^{2/3}$ finite size correction: In the spin glass phase the leading finite size correction is the same for the binary and Gaussian couplings. Systems of sizes N from 128 to 1024 have been simulated with 128 disorder samples for each system size (but for $N = 1024$, where I used 196 samples). The integration over t was done with the trapezoidal rule, with 39 non uniformly spaced points¹⁷. Integrating with only half of the points makes a very small effect on the integrand (smaller than the estimated statistical error). The data presented at T_c (Fig. 9 and 12) include the results of an additional simulation of a system with $N = 2048$ sites, limited to the paramagnetic phase, with $T \in [1.0, 1.3]$, $\Delta T = 0.025$, with 128 disorder samples, and a 15 points discretization of t .

In the low T phase, a remarkable scaling is observed if one plots the ratio $\mathcal{D}(t)/\mathcal{D}(t=0)$ as a function of $tN^{2/3}$, as shown in Fig. 8. It means that, to a good approximation, one has $\mathcal{D}(t)/\mathcal{D}(0) = F(tN^{2/3})$, with the function $F(x)$ decaying faster than $1/x$ for large x , making the integral in (73) converge. One has accordingly in the low T phase $f_N - f_\infty \propto 1/N^{2/3}$.

The situation is different at T_c , as shown in Fig. 9, the ratio $\mathcal{D}(t)/\mathcal{D}(t=0)$ scales with a different exponent, namely like $F(tN^{1/3})$, with a large x behavior compatible¹⁸ with $F(x) \propto 1/x$, then

$$\begin{aligned}
 f_N(T) - f_{N/2}(T) &\propto \int_0^1 dt \mathcal{D}(t) = \mathcal{D}(0) \int_0^1 dt F(tN^{1/3}) \\
 &\propto 1/N \ln N/N_0,
 \end{aligned}
 \tag{75}$$

¹⁷ With a distribution adapted to the shape of $\mathcal{D}(t)$, that is peaked at low t .

¹⁸ Admittedly much larger system sizes would be needed in order to be sure that the system really obeys this asymptotic behavior.

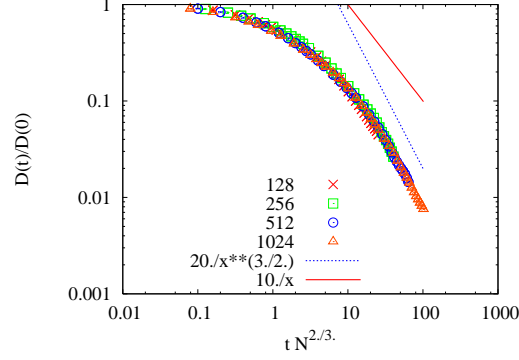


Fig. 8. $\mathcal{D}(t)/\mathcal{D}(t=0)$ as a function of $tN^{2/3}$ (both in logarithmic scale), for $T = 0.6$. The full line shows the $1/x$ behavior, the dotted line shows the $1/x^{3/2}$ behavior. Clearly $\mathcal{D}(t)$ decreases faster than $1/x$ for large x . The precise behavior of $\mathcal{D}(t)$ is not essential for my argument, as soon as $\mathcal{D}(t)$ decays faster than $1/x$.

for some undetermined N_0 . Use has been made of the fact that, according to finite size scaling, $\mathcal{D}(0) = -1/2 < (q_{1,2}^{(1)})^2 > = -1/2 < (q_{1,2}^{(2)})^2 >$ scales like $N^{2\beta/(d\nu)} \tilde{G}((T - T_c)N^{1/(d\nu)})$, with a finite non zero $\lim_{x \rightarrow 0} \tilde{G}(x)$ and that $\beta/(d\nu) = 2/3$ (see Subsec. 2.4). This behavior of $f_N(T) - f_{N/2}(T)$ is in agreement¹⁹ with (70).

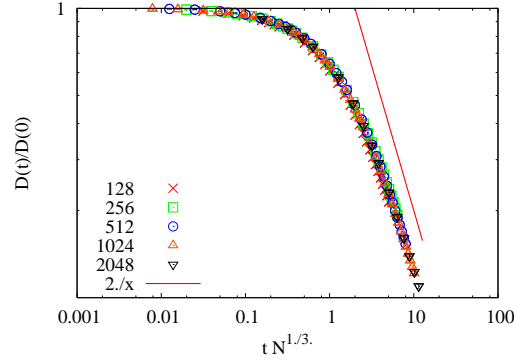


Fig. 9. $\mathcal{D}(t)/\mathcal{D}(t=0)$ as a function of $tN^{1/3}$ (both in logarithmic scale), for $T = T_c$. The straight line shows the expected $1/x$ behavior, in order to guide the eyes.

Figure 10 shows, as a function of $1/N^{2/3}$, my estimate at $T = 0.4$ of the difference $(f_N - f_{N/2})/T$, obtained by integrating numerically (73), compared to the result of a linear fit $(f_N - f_{N/2})/T = -A/N^{-2/3}$, with $A = 0.82 \pm 0.02$

¹⁹ But the value of the prefactor is not predicted by my method.

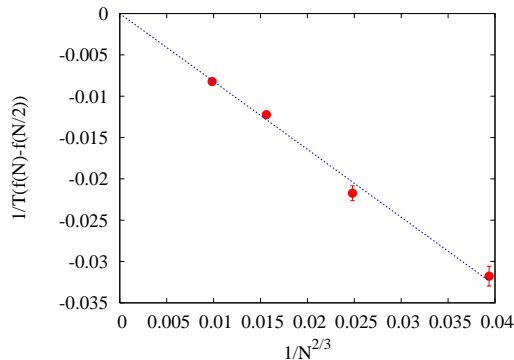


Fig. 10. Numerical data for $(f_N - f_{N/2})/T$ as a function of $1/N^{2/3}$, together with a numerical fit to the data of the form $(f_N - f_{N/2})/T = -A/N^{2/3}$, with $A = 0.82 \pm 0.02$ dotted line. Here $T = 0.4$, $N = 128, 256, 512$ and 1024 .

and $\chi^2 = 4.9$. The agreement is good within estimated statistical errors. A similar agreement is obtained for other values of T in the spin glass phase, e.g. $A = 0.39 \pm 0.01$ with $\chi^2 = 3.6$ for $T = 0.6$, and $A = 0.18 \pm 0.01$ with $\chi^2 = 33$ (a large value presumably related to the proximity of the critical point) for $T = 0.8$. The value $\omega = 2/3$ is in contradiction with the old analytical prediction of [66]. In this paper, arguments are given that relate ω to the exponent p of the first correction term in the expansion of the replicated free energy $-1/\beta \lim_{N \rightarrow \infty} 1/N \ln \overline{Z^n_{\mathcal{J}}}$ in powers of n , by the equation $\omega = (p-1)/p$. In the paramagnetic phase it is known that there is no term in this expansion beyond the linear term, i.e. p is infinite, and thus $\omega = 1$ in agreement with the previous discussion. In the spin glass phase Kondor [67] has found, using the truncated model of (56), that $p = 6$, and thus $\omega = 5/6$. The resolution of this contradiction lays presumably in the use of the Parisi approximation (58) in [67], and we can conjecture from our data that indeed $p = 3$.

Since the energy at zero temperature (and thus the free energy) also behaves like $1/N^{2/3}$, the most natural conclusion is that the leading finite size corrections for both $f_N(T)$ and $e_N(T)$ behave like $1/N^{2/3}$ in the whole low temperature phase, for both binary and Gaussian distributions. This seems however to contradict the numerical results of [68]. In this paper, the internal energy of the SK model with Gaussian $P(\mathcal{J})$ has been measured with Monte Carlo simulations for values of T between $T = 0.1$ (a very low value made possible by the small sizes simulated) and $T = 1.22$, with $N = 36, 64, \dots, 196$. The data for $e_N(T)$ are fitted²⁰ as $e_N(T) = e(T) + a(T)N^{-\omega}$, with a result for ω that is compatible with $2/3$ for both $T = 0$ and $T = T_c$, but with a pronounced deep between, in contradiction with my conjecture. Using the data for $e_N(T)$ obtained from the simulation of [9], it is quite simple to repeat the

²⁰ Using the precise estimates of $e(T)$ from [30].

analysis of [68] for systems up to $N = 4096$ (but with binary $P(\mathcal{J})$). Figure 11 shows my results compared to the one of [68]. The use of larger system sizes clearly reduce the effect observed in this paper. The most likely conclusion is that the analysis of [68] is affected by systematic errors due to the small sizes used. The shape of the sub-leading corrections to the energy is not known below T_c , it is known at the critical point, however, and there the sub-leading corrections are decaying very slowly, the expansion is indeed an expansion in powers of $N^{-1/3}$, and it is may be not so surprising to have difficulties finding the correct leading exponent from data with $36 \leq N \leq 196$.

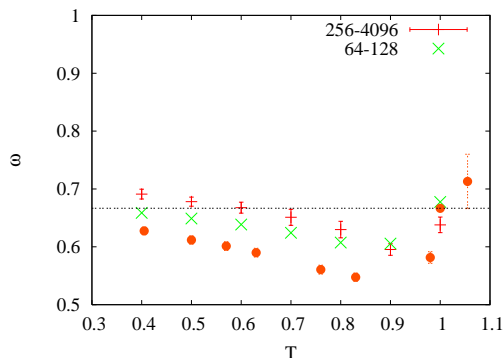


Fig. 11. Behavior of the finite size exponent ω as a function of temperature for the Sherrington–Kirkpatrick model. From top to bottom: results of a (gnuplot) fit of the data of [9] with $4096 \geq N \geq 256$ (with estimated errors); fit of the same data with $128 \geq N \geq 64$ (without estimated errors, in order not to clutter the figure) and data from [68].

Figure 12 shows my estimates for $(f_N - f_{N/2})/T$ at T_c as a function of $1/N$, together with the prediction of (70). A good agreement (with $\chi^2 = 4.3$ if one excludes the $N = 128$ data from the fit) is obtained using the value $1/N_0 = 7.8 \pm 0.2$, namely $f_{(-1)} = \ln(7.8)/12 = 0.17\dots$, within the range of results presented in [55].

The method has been extended [69] to the computation of the fluctuations of the free energy, with the result that, in the spin glass phase, $\Delta^2 f_N(T) = \overline{f_N^2(T)} - \overline{f_N(T)}^2 \propto N^{-2\sigma}$, with $\sigma \approx 3/5$. This is definitively smaller than the value found at $T = 0$ [59, 60, 61, 62, 63], that is $\sigma \approx 3/4$.

4.4 Conclusions

The picture that emerges is the following: above T_c the finite size corrections of both $f_N(T)$ and $e_N(T)$ are given by series in powers of $1/N$, whose terms can be evaluated by perturbation theory. This expansion becomes singular

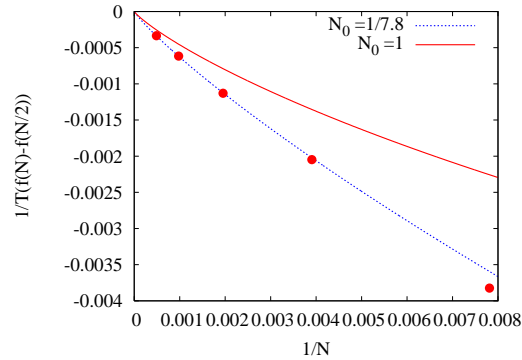


Fig. 12. Numerical data for $(f_N - f_{N/2})/T$ as a function of $1/N$, together with the behavior implied by the equation: $f_N/T = f_\infty/T + 1/(12N) \ln N/N_0$. The full line is drawn with the value $N_0 = 1$. The dotted line is drawn with the value $1/7.8$, from a fit to the data. Here $T = 1$, $N = 128, 256, \dots, 2048$.

as the critical point is approached. At the critical point the size dependent part of the free energy behaves like $(1/12N) \ln N/N_0$ and the size dependent part of the internal energy as $e_{(-2/3)}/N^{2/3}$, with coefficients that are poorly determined analytically, but can be evaluated with Monte Carlo simulation. The sub-leading corrections are decaying very slowly with N . In the spin glass phase, the data are compatible with a $1/N^{2/3}$ behavior for both the leading finite size corrections to $e_N(T)$ and $f_N(T)$.

5 Acknowledgments

I thank Wolfhard Janke for organizing this very pleasant CECAM workshop. My interest in the Sherrington–Kirkpatrick model stems from a continued collaboration with Enzo Marinari, which I thank warmly. The $H \neq 0$ data have been obtained in collaboration with Barbara Coluzzi. I also thank Andrea Crisanti and Tommaso Rizzo and Helmut Katzgraber, and Ian Campbell for providing me with their numerical data, and Giulio Biroli, Jean-Philippe Bouchaud, Cirano de Dominicis and Tamàs Temesvári for discussions. I am deeply indebted to Giorgio Parisi for many insights.

References

1. S.F. Edwards and P.W. Anderson: J. Phys. **F5**, 965 (1975).
2. D. Sherrington and S. Kirkpatrick: Phys. Rev. Lett. **35**, 1792 (1975); Phys.Rev. **B17**, 4384 (1978).
3. W. L. McMillan: J. Phys. **C17**, 3179 (1984); A. J. Bray and M. A. Moore: J. Phys. **C18**, L699 (1985); D. S. Fisher and D. A. Huse: Phys. Rev. **B38**, 386 (1988).

4. G. Parisi: Phys. Lett. **73A**, 203 (1979).
5. G. Parisi: J. Phys. **A13**, L115 (1980).
6. G. Parisi: J. Phys. **A13**, 1101 (1980).
7. G. Parisi: J. Phys. **A13**, 1887 (1980).
8. T. Rizzo and A. Crisanti: Phys. Rev. Lett. **90**, 137201 (2003); T. Rizzo: J. Phys. A. Math. Gen. **34**, (2001) 5531;
9. A. Billoire and E. Marinari: J. Phys. **A 33**, L265 (2000); Eur. Phys. Lett. **60**, 775 (2002).
10. D. J. Thouless. P. W. Anderson and R.G. Palmer: Phil. Mag. **35**, 593 (1977).
11. A. Cavagna, I. Giardina and G. Parisi: Phys. Rev. Lett. **92**, 120603 (2004); T. Aspelmeier, R. A. Blythe, A. J. Bray, M. A. Moore: Phys. Rev. **B74**, 184411 (2006).
12. A. J. Bray and M. A. Moore: J. Phys. **C13**, L469 (1980); T. Aspelmeier, A.J. Bray and M. A. Moore: Phys. Rev. Lett. **92**, 087203 (2004); G. Parisi: lecture notes, Les Houches summer school (2005), cond-mat/0602349
13. K.H. Fischer and J.A. Hertz: *Spin Glasses* (Cambridge University Press, Cambridge, 1991).
14. K. Binder and A. P. Young: Rev. Mod. Phys. **58**, 4 (1986).
15. M. Mézard, G. Parisi and M. Virasoro: *Spin Glass Theory and Beyond* (World Scientific, Singapore, 1987).
16. T. Castellani and A. Cavagna: Spin-glass Theory for Pedestrians, Lecture notes of the school: *Unifying Concepts in Glassy Physics III*, Bangalore, June 2004 J. Stat. Mech. P05012 (2005).
17. D. Sherrington: *Spin Glasses*, cond-mat/9806289.
18. C. de Dominicis and I. Giardina: *Random Fields and Spin Glasses. A field theory approach* (Cambridge University Press, Cambridge, 2007).
19. N. Kawashima and H. Rieger: Recent Progress in Spin Glasses, in *Frustrated Spin Systems*, ed by H.T.Diep (World Scientific, Singapore 2005).
20. E. Marinari, G. Parisi and J. Ruiz-Lorenzo: Numerical Simulations of Spin Glass Systems, in *Spin-glasses and random fields*, ed by A. P. Young (World Scientific, Singapore 1997).
21. E. Marinari, G. Parisi, F. Ricci-Tersenghi, J. Ruiz-Lorenzo and F. Zuliani: *Replica Symmetry Breaking in Short Range Spin Glasses: A Review, of the Theoretical Foundations and of the Numerical Evidence*, J. Stat.Phys. **98**, 973 (2000).
22. J.-P. Bouchaud, L. F. Cugliandolo, J. Kurchan and M. Mézard: Out of equilibrium dynamics in spin-glasses and other glassy systems, in *Spin-glasses and random fields*, ed by A. P. Young (World Scientific, Singapore 1997).
23. L. F. Cugliandolo: *Dynamics of glassy systems*, Lecture notes, Les Houches Summer school, July 2002.
24. A. Crisanti and F. Ritort: *Violation of the fluctuation-dissipation theorem in glassy systems: basic notions and the numerical evidence*, Topical Review Paper, J. Phys. **A36**, R181 (2003).
25. B. Berg, A. Billoire and W. Janke: Phys. Rev. **E66**, 046122 (2002).
26. M. Mézard, G. Parisi and M. Virasoro: Eur. Phys. Lett. **1** 77 (1986).
27. G. Parisi, Phys.Rev. Lett., **50**, 1946 (1983).
28. J. R. L. de Almeida and D. J. Thouless: J. Phys. **A11**, 983 (1978).
29. C. de Dominicis and I. Kondor: Phys. Rev. **27**, 606 (1982).
30. A. Crisanti and T. Rizzo: Phys. Rev. **E 65**, 046137 (2002).

31. A. Crisanti, T. Rizzo and T. Temesvári: Eur. Phys. J. **B33**, 203 (2003).
32. M. Mézard, G. Parisi, N. Sourlas, G. Toulouse and M. Virasoro: J. Phys. (France) **45**, 843 (1984); M. Mézard and M. Virasoro: J. Phys. (France) **46**, 1293 (1985).
33. S. Wiseman and E. Domany: Phys. Rev. **E58**, 2938 (1998).
34. F. Guerra: Int. J. of Mod. Phys. **B10**, 1675 (1996).
35. F. Guerra and F. L. Toninelli: Comm. Math. Phys. **230**, 71 (2002).
36. F. Guerra: Comm. Math. Phys., **233**, 1 (2003).
37. M. Talagrand: CRAS **337**, 111 (2003); Annals of Math., **163**, 221 (2006).
38. F. Guerra: `cond-mat/0604674`.
39. J. M. Kosterlitz, D. J. Thouless and R. C. Jones: Phys. Rev. Lett. **36**, 1217 (1976).
40. E. Gardner: Nucl. Phys. **B257**, 747 (1985); D. J. Gross and M. Mézard, Nuc. Phys. **B420** 431 (1984).
41. A. Montanari and F. Ricci-Tersenghi: Eur. Phys. J. **B33**, 339 (2003).
42. A. Crisanti and H.-J. Sommers: Z. für Physik, **B87**, 341 (1992).
43. A. Crisanti, H. Horner and H.-J. Sommers: Z. für Physik, **B92**, 257 (1993).
44. A. Billoire, L. Giomi, E. Marinari: Eur. Phys. Lett. **71**, 824 (2005).
45. K. Hukushima and K. Nemoto: J. Phys. Soc. Japan **65**, 1604 (1996); M. C. Tesi, E. J. Janse van Rensburg, E. Orlandini and S. G. Whittington: J. Stat. Phys. **82**, 155 (1996); E. Marinari: *Optimized Monte Carlo Methods in Advances in Computer Simulation*, ed by J. Kertesz and I. Kondor (Springer-Verlag 1997).
46. A. D. Sokal: *Monte Carlo Methods in Statistical Mechanics: Foundations and New Algorithms*, Lectures at the Cargèse Summer School on *Functional Integration: Basics and Applications*, September 1996.
47. J. Zinn-Justin: *Quantum Field Theory and Critical Phenomena* (3rd edition) (Clarendon, Oxford University Press, 1996).
48. Onuttom Narayan and A.P. Young: Phys. Rev. **E64**, 021104 (2001).
49. W. Kerler and P. Rehberg: Phys. Rev. **E50**, 4220 (1994).
50. H. G. Katzgraber, S. Trebst, D. A. Huse, and M. Troyer: J. Stat. Mech. P03018 (2006).
51. A. Crisanti and T. Rizzo: private communication.
52. A. Billoire and B. Coluzzi: Phys. Rev. **E68**, 026131 (2003).
53. B. N. Bhatt and A. P. Young: J. of Magnetism and Magnetic Materials, **54**, 191 (1986);
54. S. Ciliberti and E. Marinari: J. Stat. Phys. **115**, 557 (2004); G. Hed, A.P. Young and E. Domany: Phys. Rev. Lett. **92**, 157201 (2004).
55. G. Parisi, F. Ritort and F. Slanina: J. Phys. **A26**, 247 (1992).
56. G. Parisi, F. Ritort and F. Slanina: J. Phys. **A26**, 3775 (1993).
57. J. Yeo, M. Moore and T. Aspelmeier: J. Phys. **A38**, 4027 (2005).
58. M. Palassini: PhD thesis, Scuola Normale Superiore di Pisa, 2000 (unpublished).
59. M. Palassini: `cond-mat/0307713`.
60. J.-P. Bouchaud, F. Krzakala, and O. Martin: Phys. Rev. **B68**, 224404 (2003).
61. S. Boettcher: Eur. Phys. J. **B31**, 29 (2003); S. Boettcher: Eur. Phys. J. **B46**, 501 (2005).
62. H. G. Katzgraber, M. Körner, F. Liers, M. Jünger and A. K. Hartmann: Phys. Rev. **B72**, 094421 (2005).
63. K. Pál: Physica, **A367**, 261 (2006).

64. A. Andreanov, F. Barbieri and O. Martin: Eur. Phys. J. **B41**, 365 (2004).
65. A. Billoire: Phys. Rev. **B73**, 132201 (2006).
66. A. Crisanti, G. Paladin, H.-J. Sommers and A. Vulpiani: J. Phys. I (France) **2**, 1325 (1992).
67. I. Kondor: J. Phys. **A16**, L127 (1983).
68. H. G. Katzgraber, and I. A. Campbell: Phys. Rev. **B68**, 180402(R) (2003).
69. M. Goethe and T. Aspelmeier, cond-mat/0610028.